

# Preparation and characterization of PAN nanofibers containing boehmite nanoparticles for the removal of microbial contaminants and cadmium ions from water

Sedigheh Borhani, Arezo Asadi and Hossein A. Dabbagh

## ABSTRACT

Nanofibers of polyacrylonitrile (PAN)/boehmite were prepared by electrospinning a homogeneous solution of PAN/DMF (dimethyl formamide). Enhancing the amount of boehmite nanoparticles (NPs) led to increase in the nanofibers' diameter. Samples had high pure water flux, which did not change significantly with boehmite concentration, but decreased with increasing electrospinning duration. *Escherichia coli* bacteria removal was remarkably more efficient, as it was enhanced from 72.33% to 97.37% with increase in the boehmite NPs' concentration from 0 to 10% wt. High bacterial removal efficiency could be attained by the large surface area of NPs, as well as the electrostatic force of attraction between NPs and microorganisms. The increase in boehmite concentration from 10 to 30 and 50% did not noticeably affect bacterial removal. Prolonging electrospinning time significantly enhanced bacteria removal. Hence, it was shown that 6-hour electrospinning of PAN/boehmite nanofiber layers composed of 50% boehmite led to 99.7%, 99.39%, 99.8%, and 74% *E. coli*, *Staphylococcus aureus* bacteria removal, particles' separation efficiency of 2  $\mu\text{m}$  and cadmium adsorptivity, respectively, which were better than those obtained by using pure PAN nanofibers. *E. coli* bacterial removal efficiency of the sample was increased to 99.99% by repeating filtering four times. Considering the results, this PAN/boehmite nanofibers' membrane has potential application to purification of drinking water.

**Key words** | antibacterial, boehmite NPs, cadmium, nanofibers, water filtration

Sedigheh Borhani (corresponding author)

Arezo Asadi

Department of Textile Engineering,  
Isfahan University of Technology,  
Isfahan 84156-83111,  
Iran  
E-mail: sborhani@iut.ac.ir

Hossein A. Dabbagh

Department of Chemistry,  
Isfahan University of Technology,  
Isfahan 84156-83111,  
Iran

## INTRODUCTION

Water is the most vital substance as its lack or deficiency seriously threatens human life and health. Access to water without chemical contaminants and pathogens is necessary for human health. Bacterial infections such as cholera, dysentery, and typhoid account for the majority of common waterborne diseases, leading to millions of deaths all over the world. In particular, pathogenic bacteria existence, lack or excessive amounts of necessary ions, suspended particles, and water taste and smell are the dominant concerns related to potable water (Kumar & Pandit 2012). Also, heavy metals such as lead, copper, arsenic, mercury, and cadmium in drinking water have harmful effects on human health (Song *et al.* 2011).

doi: 10.2166/wh.2020.110

Water disinfection methods include chemical and physical agents, radiation, and mechanical devices. Regarding bioenvironmental and economic issues, neither chemical agents nor radiation method can be recommended for water disinfection (Savage & Diallo 2005; Li *et al.* 2008; Botes & Eugene 2010). Nowadays, the absorption method has attracted a great deal of attention in the field of pollutant removal owing to both high-quality and cost-effectiveness. This procedure is largely affected by various parameters such as pollutant and absorbent interaction, surface area and particle size of the absorbent, pH, and contact duration (Kumar & Pandit 2012). Although filtration is known as the most conventional and practical method for biological

pollutants' removal, it involves two serious challenges: (1) the high efficiency of pollutants' removal is obtained by a large pressure drop and (2) the aggregated biological residues are likely to pass through tiny pores, contaminating the filtrate (Fiksdal & Leiknes 2006; Li *et al.* 2009). Tremendous progress in nanoscale science and engineering has made a breakthrough in improving water filtration (Savage & Diallo 2005; Pendergast & Hoek 2011). The use of both natural and synthetic nano-materials such as chitosan, carbon nanotube, and fullerene, as well as metallic (e.g., Ag) and metallic oxides' nanoparticles ((NPs) e.g., Al<sub>2</sub>O<sub>3</sub>, TiO<sub>2</sub>, ZnO, CuO), has been reported in many studies as antimicrobial NPs to filter water (Li *et al.* 2008; Botes & Eugene 2010). Mpenyana-Monyatsi *et al.* (2012), for example, showed the *E. coli* antibacterial characterization of all samples prepared by the precipitation of silver NPs on different beds such as zeolite, sand and cation, and anion resin. Moreover, Phong *et al.* (2009) documented 100% *Escherichia coli* (*E. coli*) and *Bacillus subtilis* bacteria removal by covering a flexible foam of polyurethane with silver NPs. Song *et al.* (2011) investigated the removal of heavy metal ions (Hg, Cd, Mn, and Cr) from aqueous solution using polyrhodanine-encapsulated  $\gamma$ -Fe<sub>2</sub>O<sub>3</sub> NPs. They found that the magnetic polyrhodanine NPs are recyclable adsorbents and can be used to remove hazardous heavy metals from wastewater. Research works have also demonstrated alumina capability in decreasing or removing metal ions and viral pollutants (Hota *et al.* 2008; Brown & Sobsey 2009; Noordin & Liew 2010). Alumina is an umbrella term encompassing aluminum oxide (Al<sub>2</sub>O<sub>3</sub>), aluminum hydroxide, such as aluminum oxihydroxide (AlOOH), and aluminum trihydroxide (Al(OH)<sub>3</sub>) (Noordin & Liew 2010). Being a relatively cheap, non-toxic, stable and chemical resistant, alumina has a broad range of applications, as a thermal insulator, a catalyst, a reinforcement agent, and a fire protector (Shackelford & Doremus 2008). Alumina NPs, due to the unique property of positively charged surface, can be regarded as a potentially more suitable filter. This is due to the fact that the electrostatic force of attraction is well established between positively charged NPs and negatively charged hydroxyl and phosphate groups in microorganisms (Pal *et al.* 2006; Li *et al.* 2009). Many industries including filtration can benefit from the exclusive properties of nanofibers. Nanofibers are usually produced using electrospinning which is a simple

and low cost method. High surface area, tiny and interconnected pores, chemical activities, light, and ultrathin layers of nanofibers have noticeably improved filtration efficiency. In particular, high porosity, integrated pores, and functionalization of nanofibers have turned them into the top priority in the air (aerosol) and liquid filtration industry (Gibson *et al.* 2001; Kozlov *et al.* 2018; Cheng *et al.* 2019; Correa *et al.* 2019). Nanofibers' functionalization has been achieved by both metallic and inorganic NPs. The synergistic effect of organic-inorganic hybrid nanofibers has resulted in a vast range of applications due to some valuable properties (Cheng *et al.* 2019; Correa *et al.* 2019).

Different techniques used for alumina nanofibers' production, such as electrospinning, sol-gel, and mercury-mediated and chemical vapor deposition in flame, have been extensively reported (Panda & Ramakrishna 2007; Teoh *et al.* 2007; Yang *et al.* 2009; Noordin & Liew 2010). Furthermore, filtration performance in removing bacterial pollutants and heavy metal ions has been evaluated in many studies (Hota *et al.* 2008; Brown & Sobsey 2009; Li *et al.* 2009; Noordin & Liew 2010). Despite numerous studies conducted on filters made of alumina nanofibers, there are few investigations on using alumina NPs-containing nanofibers (polymer nanofiber/ceramic). Boehmite (AlOOH) or hydrated alumina (aluminum hydroxide) is an intermediate produced in the alumina synthesis procedure with many hydroxyl groups attached on the surface, helping it to be largely used as an absorbent and a catalyst (Vatanpour *et al.* 2012; Karger-Kocsis & Lendvai 2018). The results obtained by the study of Li *et al.* (2009) on alumina nanofibers confirmed the viral aerosol agent removal, indicating better efficiency and less pressure drop, as compared to high-efficiency particulate air (HEPA) filters. Hota *et al.* (2008) also electrospun boehmite NPs-containing nylon 6 and polycaprolactone nanofibers, showing cadmium adsorption in both hydrophobic and hydrophilic polymers. The large bacterial removal of boehmite NPs can encourage scientists to develop filtration methods. The above-mentioned studies have shown that nanofibers and boehmite NPs are superior to conventional membranes and chemical disinfectants (e.g., chlorine) due to their high surface area, as well as the ability to eliminate bacteria and heavy metals from water without formation of toxic by-products. Therefore, the objective of this paper is to investigate the filtration and bacterial

removal efficiency of electrospun PAN/boehmite nanofibers on carbon-coated polyurethane foam as the substrate, for removal of *E. coli* and cadmium ion in water. The effect of boehmite NPs' concentration and the electrospinning duration of PAN/boehmite nanofibers on their performance were evaluated.

## METHODS

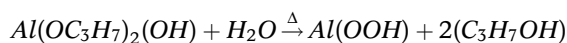
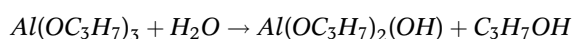
### Materials

Polyacrylonitrile (PAN) with an average molecular weight of 70,000 g/mol was obtained from Polyacryl Co., Isfahan (Iran). Dimethyl formamide (DMF) was purchased from Merck as the solvent for the PAN. *E. coli* (ATCC 35218), as a kind of Gram-negative bacteria, *S. aureus* (ATCC 29213) as a kind of Gram-positive bacteria, were used for antibacterial evaluation. Aluminum isopropoxide (Al [OCH (CH<sub>3</sub>)<sub>2</sub>]<sub>3</sub>, 98%) and cadmium chloride were supplied by Merck (Germany) and used as the precursors for the synthesis of boehmite and the Cd (II) ions' solution, respectively. Deionized water was used throughout the experiments.

### Boehmite preparation procedure

The sol-gel technique was used for the preparation of boehmite NPs, based on the method described by Dabbagh & Shahraki (2013). To describe it briefly, water hydrolysis of

aluminum isopropoxide with 1:10 molar ratio took place at 85 °C with continuous mechanical stirring and 1-hour ultrasonic stirring at a power of 70 W, 40 kHz. The latter led to the formation of a homogeneous suspension. Then, the reaction was followed by refluxing for 24 hours. Finally, the homogeneous suspension was heated at 120 °C for 24 hours to remove the formed alcohol and the excess water. The reactions of AlOOH formation can be simplified, as shown by the following chemical equations (Teoh et al. 2007):



### Electrospinning of PAN/boehmite nanofibers

PAN/boehmite nanofibers were fabricated by using the electrospinning method. Figure 1 shows the schematic of the electrospinning setup. It is described here: first, different amounts of boehmite NPs (5, 10, 30, and 50% wt) were dispersed in DMF under ultrasonic stirring for 20 min and at a power of 70 W, 40 kHz. Next, the accurately weighed PAN (12% wt) was added to the above suspension and the polymer solution was magnetically stirred for 24 hours at room temperature.

A 1 mL syringe fitted with a metallic needle having an inner diameter of 0.7 mm was used to extrude the polymer

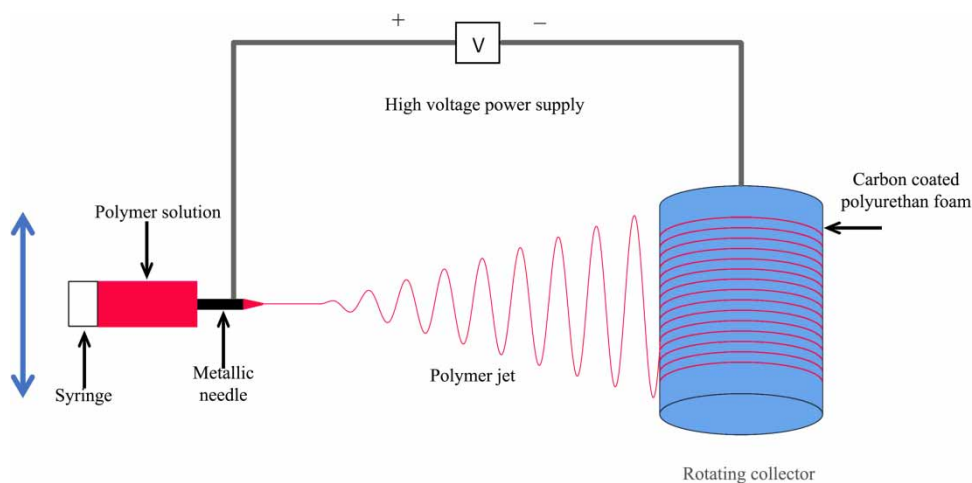


Figure 1 | The schematic of the electrospinning setup.

solution. The electrospun fibers were collected as a non-woven web on a cylinder whose surface was covered with carbon-coated polyurethane foam; this was done to not only supply appropriate mechanical properties, but also to allow pleating filter production. The electrospinning conditions of the polymer solutions were adjusted based on the production of bead-free and uniform nanofibers. The flow rate and electrospinning distance were fixed at 0.35 mL/h and 15 cm, respectively. The applied voltage of polymer solutions is provided in Table 1. The collector rotation speed and the traverse speed of the pump were 75 rpm and 4 cm/min, respectively, in order to uniformly coat nanofibers on the carbon-coated polyurethane foam. Electrospinning was performed for 2, 4, and 6 hours at ambient temperature (25 °C).

### Measurements and characterization

X-ray diffraction (XRD), which was performed by Xpert MPD with CuK $\alpha$  radiation ( $\lambda = 1.54 \text{ \AA}$ ) at a range of  $2\theta = 10\text{--}100^\circ$ , made it possible to characterize phase purity and the average particle size of the synthesized boehmite. Fourier transform infrared (FTIR) spectroscopy studies were also performed on the samples using a Bomem MB – Series 100 spectrometer (Canada), in the range of  $400\text{--}4,000 \text{ cm}^{-1}$ , by employing the KBr disk method. Nanofibers' morphology investigation was conducted by a Hitachi-S-4160 field emission scanning electron microscope (FE-SEM) and Philips EM 208S transmission electron microscope ((TEM) The Netherlands). The nanofibers' diameter was obtained from an average of 100 measurements. The viscosity of PAN/boehmite solutions was measured using a Brookfield DVII + Pro viscometer (USA) at 25 °C.

**Table 1** | Polymer solution properties and the diameter of PAN/boehmite nanofibers

| Sample | Boehmite concentration (%) | Voltage (kV) | Viscosity (Pa.s) | Diameter (nm) |
|--------|----------------------------|--------------|------------------|---------------|
| PAN    | 0                          | 17           | 0.765            | 191 ± 34      |
| PAN5   | 5                          | 17           | –                | –             |
| PAN10  | 10                         | 18.5         | 0.780            | 215 ± 56      |
| PAN30  | 30                         | 19           | 0.935            | 235 ± 46      |
| PAN50  | 50                         | 20           | 1.728            | 322 ± 47      |

### Evaluation of bacterial removal efficiency

Filtration and bacterial removal efficiency was tested against *E. coli*, an indicator for fecal water contamination, by using the dead-end test method (Lemma et al. 2015). Nutrient broth and nutrient agar were used as the liquid and solid growing medium, respectively. All test samples and glassware were sterilized in an autoclave at 120 °C for 15 min. *E. coli* was cultivated in a nutrient broth by incubating it for 24 hours at 37 °C. 500 mL of *E. coli* suspended in distilled water with a concentration of  $1 \times 10^5$  colony forming units (CFU)/mL of bacteria was passed through circular PAN/boehmite nanofiber swatches (with 50 mm diameter). The pour plate method was used to enumerate bacterial colonies on agar plates. For this purpose, 1 mL of the filtered water was poured on a nutrient agar in a Petri dish and incubated at 37 °C for 24 hours. The number of bacteria colonies formed on the agar plate for each sample was counted. The bacterial removal efficiency was determined by considering the percentage of reduction in the number of bacteria; this was based on using the following equation:

$$R\% = \frac{N_1 - N_2}{N_1} \times 100 \quad (1)$$

where  $R$  is the percentage of bacteria reduction,  $N_1$  is the number of bacterial colonies in the feed, and  $N_2$  represents the number of bacteria colonies in the filtrate. In addition, bacterial removal efficiency of the PAN50 sample, which was electrospun for 6 hours, was tested against *S. aureus* as a Gram-positive bacteria by the same procedure described for *E. coli*.

### Cd (II) ions adsorption experiments

An approach to measure cadmium ion adsorption was offered by Hota et al. (2008). This same approach was employed in this research work. A Cd (II) ion solution (5 ppm) was prepared by dissolving an exact amount of cadmium (II) chloride in double distilled water. 0.2 g of PAN/boehmite nanofibers was mixed in 20 mL of Cd (II) ions solution and shaken for 60 min. The pH value was maintained at 4 by adding ammonium hydroxide. After the separation of nanofibers from the solution by filtration, Cd (II) ion

concentration was measured by flame atomic absorption spectrometer (Perkin Elmer, Analyst 700). The adsorptivity and adsorption capacity of the samples were calculated by the following equations, respectively (Song et al. 2011):

$$q = \frac{C_o - C}{C_o} \times 100 \quad (2)$$

$$q_e = \frac{(C_o - C) \times V}{W} \quad (3)$$

where  $q$  denotes adsorptivity (%),  $q_e$  stands for adsorption capacity (mg/g),  $C_o$  and  $C$  are Cd (II) ion concentrations (mg/L) before and after adsorption,  $V$  denotes the solution volume (L), and  $W$  is the weight of nanofibers (g).

### Permeation experiment

Air permeability is the important parameter of nanofiber mats, especially for filtration applications. The thickness, porosity, and pore size of the nanofiber mat can significantly influence air permeability (Kaur et al. 2012). The total volumetric flow rate,  $Q$ , (mL/s) of PAN nanofiber mats was measured by using a Shirley permeation analyzer when pressure drop across mats, ambient temperature, and relative humidity was 100 Pa, 23 °C and 45%, respectively. Air permeability was calculated by dividing  $Q$  by the sample test area. Permeation flux experiment was carried out on a total volume of 200 mL pure water passing through the circular membrane 40 mm in diameter, at transmembrane pressure of 1 bar, in a dead-end method. The pure water flux (L/m<sup>2</sup>·h) was calculated by the following equation:

$$Flux = \frac{V}{A \cdot t} \quad (4)$$

where  $V$  is the permeated volume of pure water (L),  $A$  is the sample effective area (m<sup>2</sup>), and  $t$  is time needed to permeate 200 mL pure water through the sample (h).

## RESULTS AND DISCUSSION

### Characterization of boehmite nanoparticles

The XRD analysis result of boehmite nanoparticles (NPs) is shown in Figure 2; it was also compared with the available

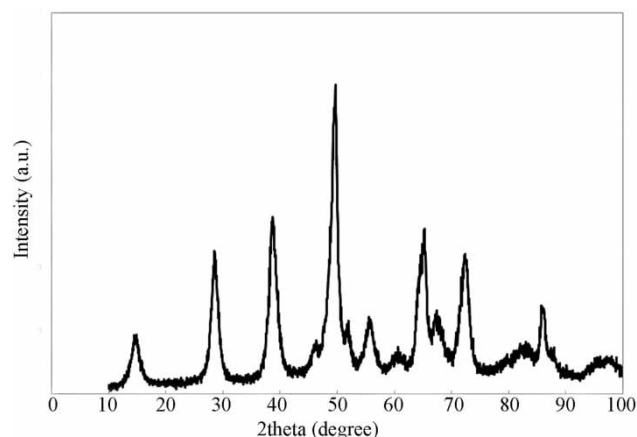


Figure 2 | XRD pattern of boehmite NPs.

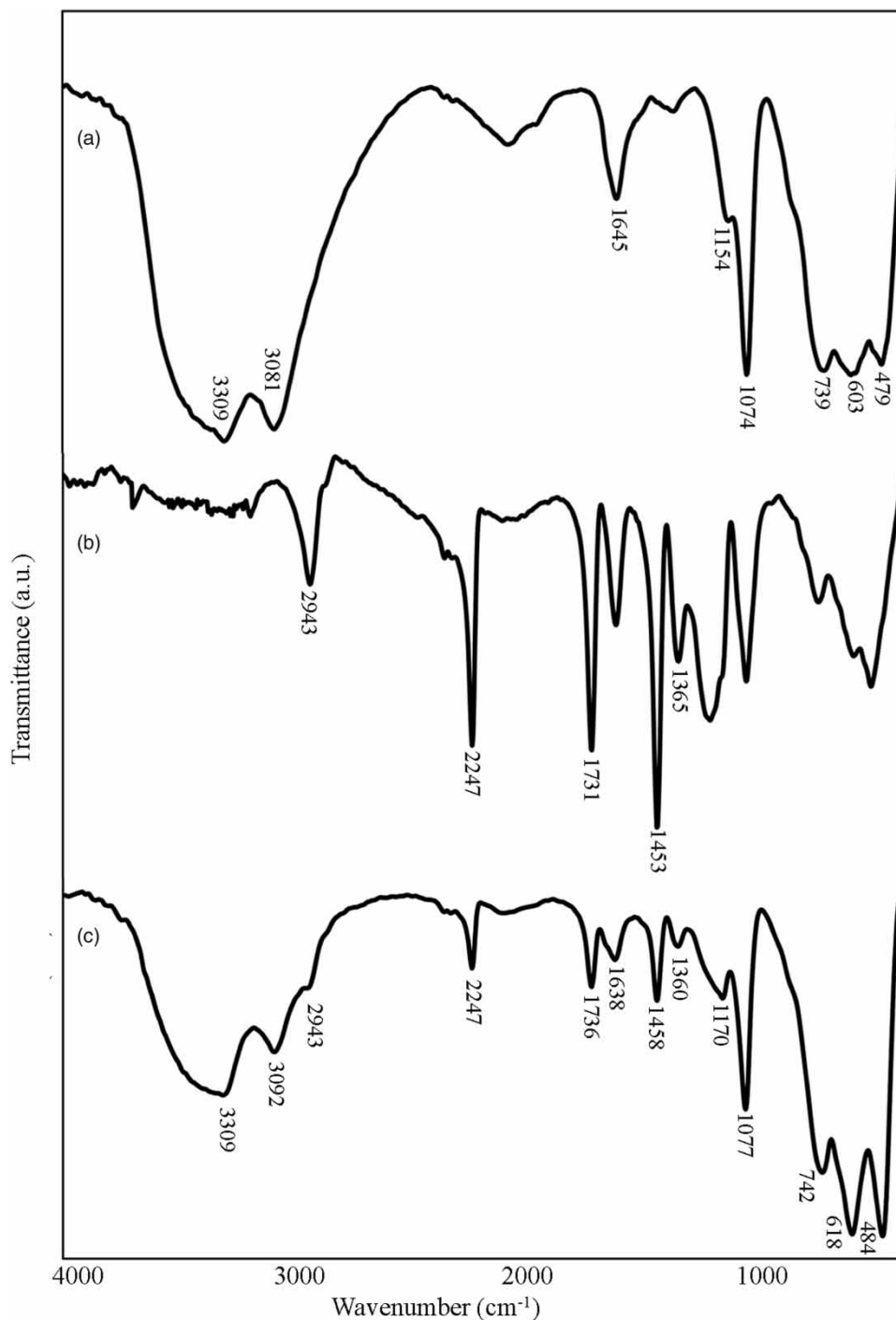
XRD data in the literature (Santos et al. 2009). The XRD pattern of the analyzed sample proved it to be an excellent mat for the poorly crystallized boehmite (pseudoboehmite). The three angles reflection in  $2\theta = 10\text{--}40^\circ$  differed slightly in broadening and significantly in their intensity in the case of the poorly and well-crystallized boehmite. For the pseudo-boehmite, notably, the lower intensity, broadening of the reflection, and a higher  $d$  value at  $2\theta = 14.6^\circ$ , which corresponded to the (020) plane, were observed, as reported in the literature (Santos et al. 2009). Thus, XRD data confirmed the successful synthesis of the poorly crystallized boehmite NPs (pseudoboehmite). According to the Debye-Scherrer equation, the average particle size was approximately 12.34 nm.

Figure 3(a) shows the FTIR spectra of boehmite NPs. The strong and well-resolved bands at 3,305 and 3,081 cm<sup>-1</sup> characterized a well-crystallized boehmite; it could be attributed to (Al)O-H asymmetrical and symmetrical stretching vibrations, respectively. Al-O-H asymmetrical and symmetrical stretching of boehmite corresponded to the bands at 1,154 and 1,074 cm<sup>-1</sup>, respectively. The peaks at 739 and 603 cm<sup>-1</sup> were due to the OH torsional mode of boehmite. The FTIR analysis results were consistent with the XRD results, thereby confirming that the crystalline phase of the prepared NPs was boehmite (Boumaza et al. 2009; Dabbagh & Shahraki 2013).

### Characterization of PAN/boehmite nanofibers

To prove the presence of boehmite NPs within the nanofibers, the FTIR and TEM analyses of PAN and PAN/boehmite nanofibers were performed and results are





**Figure 3** | FTIR spectra of (a) boehmite NPs, (b) PAN nanofiber, and (c) PAN/boehmite nanofiber with 50% wt boehmite.

depicted in Figures 3 and 4. The nanofibers' TEM image shows the presence of a large number of boehmite NPs that are evenly distributed in the prepared PAN nanofibers.

The TEM image also shows that the boehmite NPs have a rod shape structure. The FTIR spectrum of PAN (Figure 3(b)) showed characteristic absorption bands such as C-H

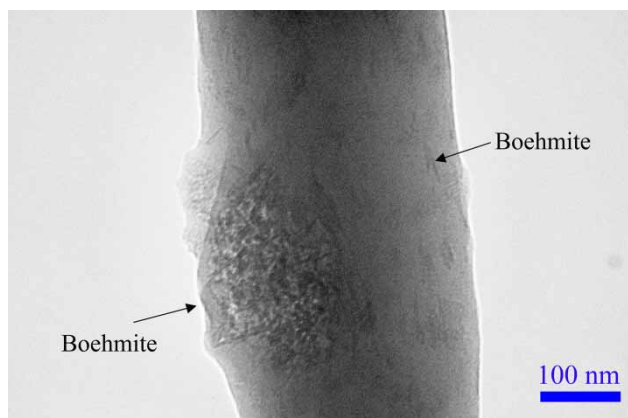


**Figure 4** | TEM micrographs of PAN nanofibers including 50% wt boehmite.

stretching vibrations at  $2,943\text{ cm}^{-1}$  and C-N stretching vibrations at  $2,247\text{ cm}^{-1}$ . The absorption band at  $1,453\text{ cm}^{-1}$  was associated with the C-H bending vibration (Foroozmehr *et al.* 2015). According to Figure 3(c), the characteristic absorption bands of boehmite ( $484, 742, 1,077, 1,170, 3,092,$  and  $3,309\text{ cm}^{-1}$ ) were present in the FTIR spectra of PAN/boehmite nanofibers, thereby confirming that boehmite NPs had been successfully incorporated in PAN nanofibers. Furthermore, lack of shift or change in absorption wavenumbers indicated the absence of the chemical interaction between PAN and boehmite NPs in the produced nanofibers.

The FE-SEM microstructures and the diameter distribution graph of electrospun PAN nanofibers with different boehmite NPs loadings in a 12% wt PAN polymer solution are shown in Figure 5. The rise of the nanofibers' diameter, as shown in Table 1 and Figure 5, was caused by an increase in the polymer solution viscosity due to the addition of boehmite NPs. Increasing viscosity by increasing the concentration of nanoparticles can be attributed to the adsorption and immobilization of a large amount of polymer by nanoparticles (Polymer properties database 2015). The rise in boehmite content from 0 to 50% wt led to an increase in the average diameter of PAN/boehmite nanofibers from 191 to 322 nm. The size of boehmite NPs was measured to be 68 and 237 nm for boehmite loadings of 10 and 50% wt, respectively, as can be seen from FE-SEM provided in Figure 6. These results implied further agglomeration of boehmite NPs on the surface of nanofibers containing 50% wt boehmite.

The permeation performance of the nanofiber layers was evaluated by measuring the air permeability and pure water flux (Figure 7). The variations in the air permeability of PAN/boehmite nanofiber layers with different boehmite content and electrospinning duration are depicted in Figure 7(a). It could be inferred from the results that air permeability was significantly enhanced by increasing boehmite content up to 30% wt; however, increasing boehmite content to 50% wt dramatically reduced air permeability. Based on Darcy's equation, increasing air permeability is associated with a decrease in pressure drop (Gibson *et al.* 2001). It was clear that when nanofibers' diameter was increased, the inter nanofiber space (pore size) was enlarged too (Abuzade *et al.* 2012). Therefore, air permeability enhancement of samples could be attributed to the increase in the pore size of nanofiber layers. The clogged pores caused by boehmite NPs' accumulation reduced the air permeability of nanofibers containing 50% wt boehmite. It is worth noting that the thickness of the nanofiber mat was increased with electrospinning duration, resulting in the reduced pore size and air permeability reduction (Kang *et al.* 2015). Based on the literature, more porosity and larger pores could cause higher air permeability and fluxes (Kaur *et al.* 2012). Figure 7(b) shows the pure water flux of different PAN/boehmite nanofiber layers. As results show, pure water flux of nanofiber layers is high and was decreased by increasing the electrospinning durations, but did not significantly change by increasing boehmite loading.

The particles' removal efficiency was measured on PAN50 nanofibers layer, electrospun for 6 hours. As shown in Table 2, the sample has a particles' separation efficiency of over 97% for particles larger than  $0.3\text{ }\mu\text{m}$ . Particles' removal efficiency was increased with increasing particle size.

#### Evaluation of the bacterial removal efficiency of PAN/boehmite nanofiber layers

Antibacterial test results of PAN/boehmite nanofibers against *E. coli* with different boehmite concentrations and electrospinning durations are provided in Table 3. The bacterial removal efficiency of PAN/boehmite nanofibers was dramatically enhanced by the increase in boehmite content up to 10% wt. Nevertheless, further increase in boehmite

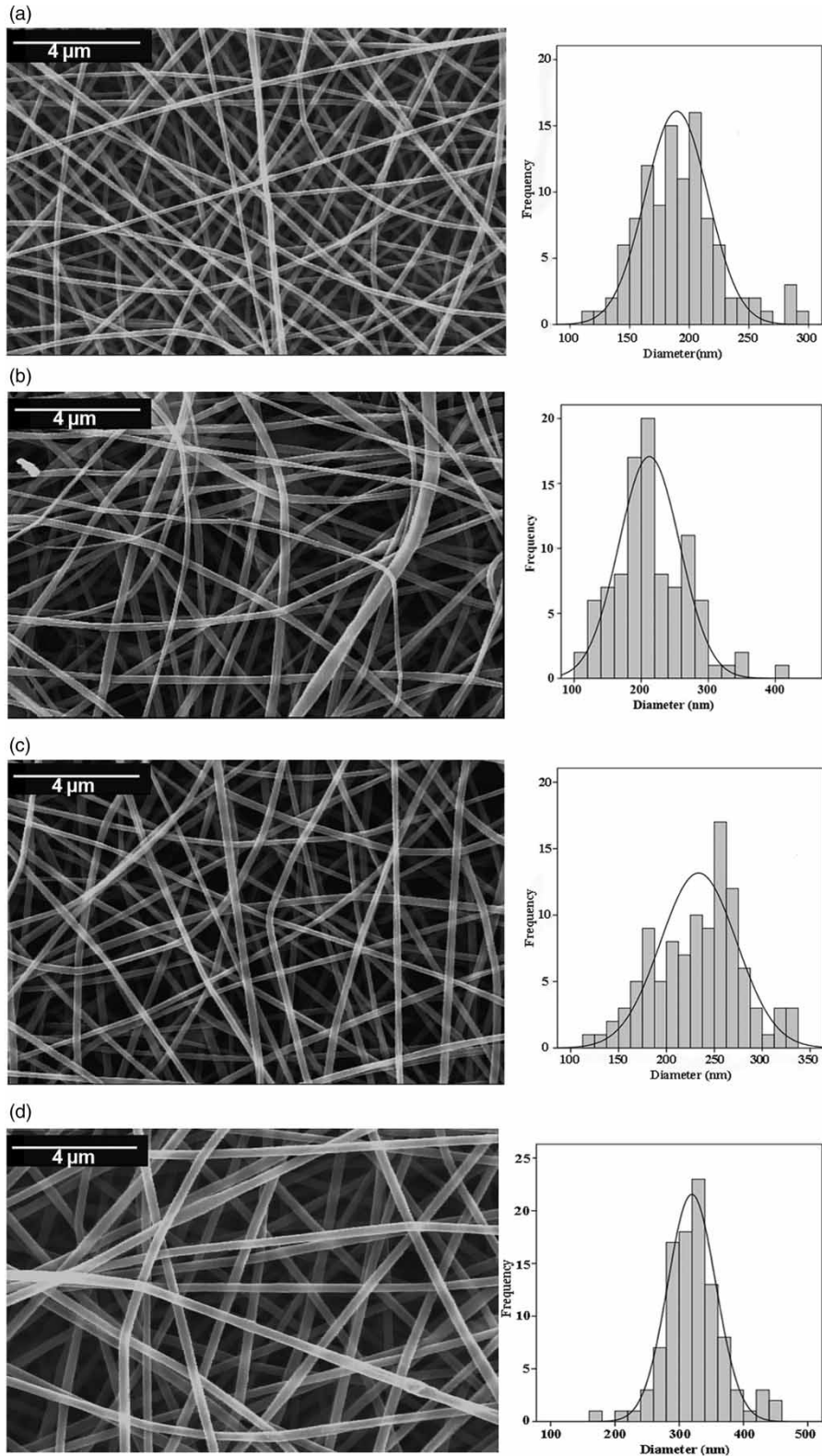


**Figure 5** | FE-SEM images and the diameter distribution curves of PAN/boehmite nanofibers including (a) 0, (b) 10, (c) 30, and (d) 50% wt boehmite.



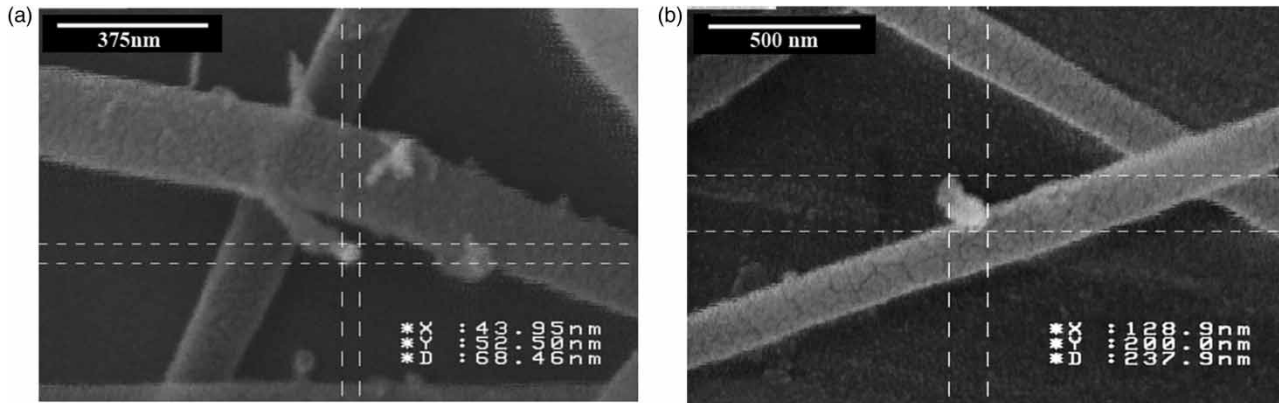


**Figure 6** | FE-SEM images of PAN/boehmite nanofibers containing (a) 10 and (b) 50% wt boehmite.

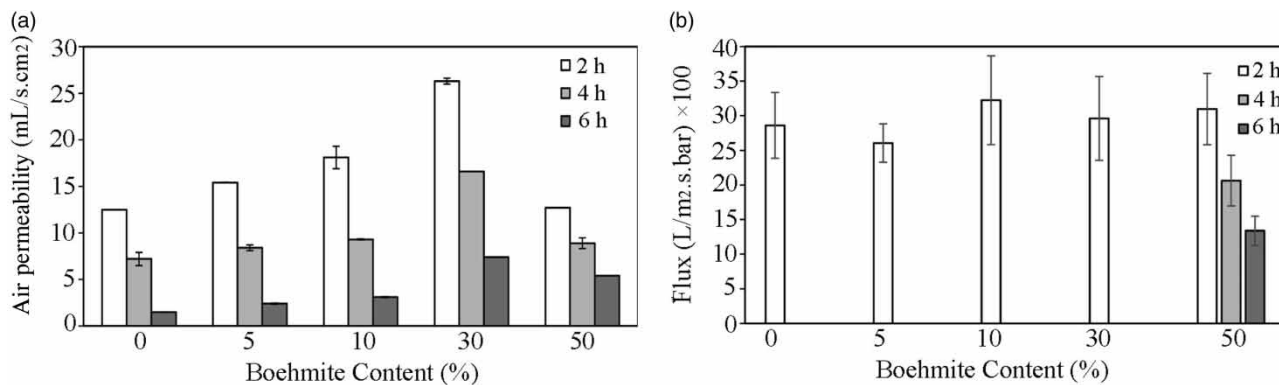


**Figure 7** | Permeation performance of PAN/boehmite nanofiber layers with different boehmite NPs and different electrospinning durations: (a) air permeability and (b) pure water flux.

**Table 2** | Particles' removal efficiency of 5, 2, and 0.3  $\mu\text{m}$  particle suspension using PAN50 sample (electrospinning time 6 hours)

| Particle size sample                             | 5.0 $\mu\text{m}$ | 2.0 $\mu\text{m}$ | 0.3 $\mu\text{m}$ |
|--|-------------------|-------------------|-------------------|
| PAN/Boehmite (50% wt) nanofiber-coated substrate | 100               | 99.8              | 97.5              |

concentration from 10 to 30 and 50% wt had no much effect on antibacterial properties. Moreover, the bacterial removal efficiency of samples was improved as the electrospinning

time enhanced, which could be regarded as a direct result of the increased nanofibers and boehmite in layers. As stated in the Introduction, the bacterial removal mechanism may be due to the electrostatic force between negatively charged microorganisms (*E. coli*) and positively charged boehmite NPs of the PAN/boehmite nanofibers (Pal et al. 2006; Li et al. 2009). To summarize, nanofiber layers of PAN/boehmite with 50% wt boehmite content exhibited higher air permeability (larger pore sizes and lower pressure

**Table 3** | *E. coli* removal efficiency of PAN/boehmite nanofibers after the first cycle

| Electrospinning time (h) | Boehmite concentration (% wt) |                  |                  |                  |                  |
|--------------------------|-------------------------------|------------------|------------------|------------------|------------------|
|                          | 0                             | 5                | 10               | 30               | 50               |
| 2                        | 72.33 $\pm$ 4.04              | 88.40 $\pm$ 2.80 | 97.37 $\pm$ 1.01 | 98.27 $\pm$ 0.95 | 99.10 $\pm$ 0.56 |
| 4                        | 79.67 $\pm$ 1.53              | 95.20 $\pm$ 0.80 | 98.70 $\pm$ 0.62 | 99.00 $\pm$ 0.66 | 99.30 $\pm$ 0.56 |
| 6                        | 88.00 $\pm$ 2.65              | 96.30 $\pm$ 1.20 | 99.20 $\pm$ 0.66 | 99.23 $\pm$ 0.31 | 99.70 $\pm$ 0.36 |

drop), better bacterial removal efficiency, suitable pure water flux, and high particles' removal efficiency.

The reuse cycles of bacterial removal efficiency were repeated four times for the PAN50 nanofibers electrospun for 6 hours and the results are shown in Figure 8(a). It should be noted that the 500 mL of *E. coli* suspended in distilled water passed through the sample four consecutive times and its bacterial removal efficiency measured after each stage, and finally, the SEM image of the filter surface was taken, as shown in Figure 8(b). According to the results, it can be concluded that by passing water from the PAN50 nanofibers more than once, the bacterial removal efficiency increases from 99.7% to 99.99%. These results show that at least four times water passage through the sample is required to reach 4-log removal of bacteria. FE-SEM micrographs (Figure 8(b) and 8(c)) of the sample surface before and after antibacterial filtration indicate that *E. coli* bacteria is captured by the PAN/boehmite nanofibers layer accompanied by no structural deformation of the nanofibers layer during filtration. To get a better idea of the spectrum of bacterial removal efficiency, the optimized sample by *E. coli* (PAN50 nanofibers electrospun for 6 hours) was tested against Gram-positive bacteria (*S. aureus*) as representative. Bacterial removal efficiency of the sample mentioned against *S. aureus* of 99.39%, was obtained, which indicates the ability of the resulting nanofibers to remove Gram-positive bacteria in addition to the Gram-negative bacteria.

### Evaluation of Cd (II) ions adsorption

The Cd (II) ion adsorption values of PAN50 nanofibers with the maximum antibacterial activity, along with pure PAN nanofibers and carbon-coated polyurethane foam, are

shown in Table 4. The results show that PAN/boehmite nanofibers had a cadmium adsorptivity of about 74% by loading 50% wt boehmite NPs. The adsorption capacity of carbon-coated polyurethane foam, PAN, and PAN/boehmite nanofibers was obtained to be 0.16, 0.20, and 0.23 mg/g, respectively, after the 60 min contact with 20 mL of the 5 ppm Cd(II) ions solution at pH = 4. Results obtained in the literature have revealed that the main mechanism of Cd (II) sorption is ion exchange; thus, carboxyl and hydroxyl functional groups could be mainly responsible for the sorption of Cd (II) (Iqbal *et al.* 2009). Hence, the cadmium absorption capability of PAN/boehmite nanofibers could be attributed to the hydroxyl groups of boehmite NPs. Hota *et al.* (2008) also reported the sorption capacity of 0.21 and 0.20 mg/g for nylon-boehmite and PCL-boehmite nanofibers containing 50% boehmite, as compared to the results obtained in the current study (0.23 mg/g).

### CONCLUSION

In this paper, the sol-gel process and the electrospinning method, as simple and cheap methods, are used to prepare PAN/boehmite nanofibers. Prepared nanofibers are characterized and are used for the removal of microbial contaminants and cadmium ions from water by using absorption as a high-quality and cost-effective method.

Both XRD and FTIR results confirmed the successful synthesis of pseudoboehmite NPs with an average particle size of about 12.34 nm. TEM observation proved that boehmite NPs were uniformly dispersed in the PAN nanofibers. The nanofibers' diameter rose due to the increase in boehmite content, which was accompanied by increased air

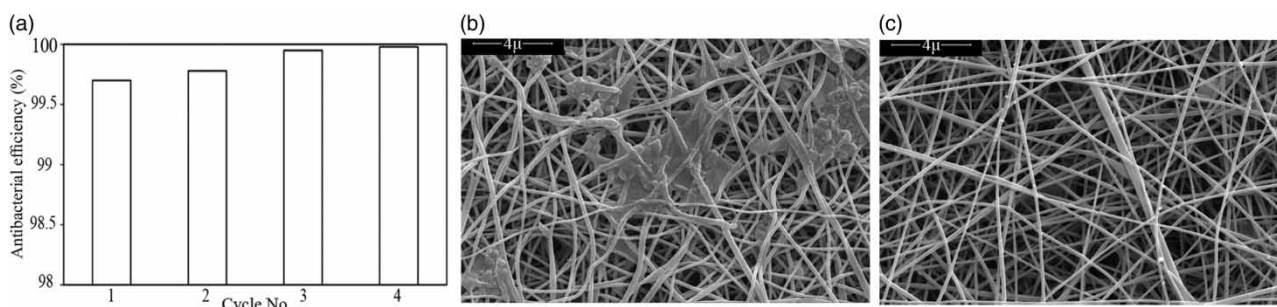


**Figure 8** | (a) *E. coli* removal efficiency cycle of PAN50 nanofibers and SEM image of the sample surface (b) after filtration, (c) before filtration.

**Table 4** | Cadmium ions' adsorption of samples

| Sample   | Adsorption capacity (mg/g) | Adsorptivity (%) |
|--|----------------------------|------------------|
| Carbon-impregnated polyurethane foam (substrate) | 0.16                       | 52.8             |
| PAN nanofiber-coated substrate                   | 0.20                       | 67.7             |
| PAN/Boehmite (50% wt) nanofiber-coated substrate | 0.23                       | 73.6             |

permeability, but the pure water flux did not change significantly. Boehmite-containing nanofiber layers were investigated to demonstrate *E. coli* bacteria removal capability through electrostatic attraction. The antibacterial property of PAN nanofiber layer was found to be directly proportional to boehmite content and the electrospinning time. A layer composed of PAN nanofibers containing 50% wt boehmite was produced through a 6-hour electrospinning process on carbon-coated polyurethane foam, and was almost better than 5, 10, and 30% wt nanofiber-containing layers in bacterial removal. Permeability of such a sample, compared to pure PAN nanofibers layer revealed that not only was bacteria removal improved to 99.99% in the presence of 50% wt boehmite, but also high permeability, structural stability, and rejecting micro particles efficiently was observed. The results also confirmed that boehmite NP-containing nanofibers were effective in cadmium (II) ions' removal in water. Based on the results of this study, it seems that electrospun PAN/boehmite layers can be recommended as a potential filter for production of safe water.

## REFERENCES

- Abuzade, R. A., Zadhoush, A. & Gharehaghaji, A. A. 2012 Air permeability of electrospun polyacrylonitrile nanoweb. *Journal of Applied Polymer Science* **126** (1), 232–243.
- Botes, M. & Eugene, C. T. 2010 The potential of nanofibers and nanobiocides in water purification. *Critical Reviews in Microbiology* **36** (1), 68–81.
- Boumazza, A., Favaro, L., Lédion, J., Sattonnay, G., Brubach, J. B., Berthet, P., Huntz, A. M., Roy, P. & Tétot, R. 2009 Transition alumina phases induced by heat treatment of boehmite: an X-ray diffraction and infrared spectroscopy study. *Journal of Solid State Chemistry* **182**, 1171–1176.
- Brown, J. & Sobsey, M. D. 2009 Ceramic media amended with metal oxide for the capture of viruses in drinking water. *Environmental Technology* **30** (4), 379–391.
- Cheng, C., Li, X., Yu, X., Wang, M. & Wang, X. 2019 Electrospun nanofibers for water treatment. In: *Electrospinning: Nanofabrication and Applications* (B. Ding, X. Wang & J. Yu, eds). Elsevier, Amsterdam, The Netherlands, pp. 419–453.
- Correa, D. S., Mercante, L. A., Schneider, R., Facure, M. H. & Locilento, D. A. 2019 Composite nanofibers for removing water pollutants: fabrication techniques. In: *Handbook of Ecomaterials* (L. M. Torres Martinez, O. V. Kkarissova & B. I. Kharisov, eds). Springer, Switzerland, pp. 441–468.
- Dabbagh, A. H. & Shahraki, M. 2013 Mesoporous nano rod-like c-alumina synthesis using phenol-formaldehyde resin as a template. *Microporous and Mesoporous Materials* **175**, 8–15.
- Fiksdal, L. & Leiknes, T. 2006 The effect of coagulation with MF/UF membrane filtration for the removal of virus in drinking water. *Journal of Membrane Science* **279** (1), 364–371.
- Foroozmehr, F., Borhani, S. & Hosseini, S. A. 2015 Removal of reactive dyes from wastewater using cyclodextrin functionalized polyacrylonitrile nanofibrous membranes. *Journal of Textiles and Polymers* **4** (1), 45–52.
- Gibson, P., Schreuder-Gibson, H. & Rivin, D. 2001 Transport properties of porous membranes based on electrospun nanofibers. *Colloids and Surfaces A: Physicochemical and Engineering Aspects* **187**, 469–481.
- Hota, G., Kumar, B. R., Ng, W. & Ramakrishna, S. 2008 Fabrication and characterization of a boehmite nanoparticle impregnated electrospun fiber membrane for removal of metal ions. *Journal of Materials Science* **43** (1), 212–217.
- Iqbal, M., Saeed, A. & Zafar, S. I. 2009 FTIR spectrophotometry, kinetics and adsorption isotherms modeling, ion exchange, and EDX analysis for understanding the mechanism of Cd<sup>2+</sup> and Pb<sup>2+</sup> removal by mango peel waste. *Journal of Hazardous Materials* **164** (1), 161–171.
- Kang, Y. O., Im, J. N. & Park, W. H. 2015 Morphological and permeable properties of antibacterial double-layered composite nonwovens consisting of microfibers and nanofibers. *Composites Part B: Engineering* **75**, 256–263.
- Karger-Kocsis, J. & Lendvai, L. 2018 Polymer/boehmite nanocomposites: a review. *Journal of Applied Polymer Science* **135** (24), 45573.
- Kaur, S., Sundarrajan, S., Rana, D., Matsuura, T. & Ramakrishna, S. 2012 Influence of electrospun fiber size on the separation efficiency of thin film nanofiltration composite membrane. *Journal of Membrane Science* **392**, 101–111.
- Kozlov, M., Moya, W. & Tkacik, G. 2018 Removal of Microorganisms From Fluid Samples Using Nanofiber Filtration Media. United States Patent 9889214, USPTO, Alexandria, VA, USA.
- Kumar, J. K. & Pandit, A. B. 2012 *Drinking Water Disinfection Techniques*. CRC Press, Boca Raton, FL, USA.
- Lemma, S. M., Esposito, A., Mason, M., Brusetti, L., Cesco, S. & Scampicchio, M. 2015 Removal of bacteria and yeast in water

- and beer by nylon nanofibrous membranes. *Journal of Food Engineering* **157**, 1–6.
- Li, Q., Mahendra, S., Lyon, D. Y., Brunet, L., Liga, M. V., Li, D. & Alvarez, P. J. 2008 Antimicrobial nanomaterials for water disinfection and microbial control: potential applications and implications. *Water Research* **42** (18), 4591–4602.
- Li, H.-W., Wu, C.-Y., Tepper, F., Lee, J.-H. & Lee, C. N. 2009 Removal and retention of viral aerosols by a novel alumina nanofiber filter. *Journal of Aerosol Science* **40** (1), 65–71.
- Mpenyana-Monyatsi, L., Mthombeni, N. H., Onyango, M. S. & Momba, M. N. 2012 Cost-effective filter materials coated with silver nanoparticles for the removal of pathogenic bacteria in groundwater. *International Journal of Environmental Research and Public Health* **9** (1), 244–271.
- Noordin, M. R. & Liew, K. Y. 2010 *Synthesis of Alumina Nanofibers and Composites*. INTECHOpen, London, UK.
- Pal, S., Joardar, J. & Song, J. M. 2006 Removal of *E. coli* from water using surface-modified activated carbon filter media and its performance over an extended use. *Environment Science Technology* **40** (19), 6091–6097.
- Panda, P. & Ramakrishna, S. 2007 Electrospinning of alumina nanofibers using different precursors. *Journal of Materials Science* **42** (6), 2189–2193.
- Pendergast, M. M. & Hoek, E. M. 2011 A review of water treatment membrane nanotechnologies. *Energy & Environmental Science* **4** (6), 1946–1971.
- Phong, N. T. P., Thanh, N. V. K. & Phuong, P. H. 2009 Fabrication of antibacterial water filter by coating silver nanoparticles on flexible polyurethane foams. *Journal of Physics: Conference Series* **187** (1), 1–8.
- Polymer properties database 2015 *Nanoparticle-reinforced Polymers*. Available from: <http://polymerdatabase.com/polymer%20physics/Nanoparticles.html> (accessed 22 July 2019).
- Santos, P. d. S., Coelho, A. C. V., Santos, H. d. S. & Kiyohara, P. K. 2009 Hydrothermal synthesis of well-crystallised boehmite crystals of various shapes. *Materials Research* **12** (4), 437–445.
- Savage, N. & Diallo, M. S. 2005 Nanomaterials and water purification: opportunities and challenges. *Journal of Nanoparticle Research* **7** (4), 331–342.
- Shackelford, J. F. & Doremus, R. H. 2008 *Ceramic and Glass Materials, Structure, Properties and Processing*. Springer, New York, USA.
- Song, J., Kong, H. & Jang, J. 2011 Adsorption of heavy metal ions from aqueous solution by polyrhodanine-encapsulated magnetic nanoparticles. *Journal of Colloid and Interface Science* **359** (2), 505–511.
- Teoh, G. L., Liew, K. Y. & Mahmood, W. A. 2007 Synthesis and characterization of sol-gel alumina nanofibers. *Journal of Sol-Gel Science and Technology* **44** (3), 177–186.
- Vatanpour, V., Madaeni, S. S., Rajabi, L., Zinadini, S. & Derakhshan, A. A. 2012 Boehmite nanoparticles as a new nanofiller for preparation of antifouling mixed matrix membranes. *Journal of Membrane Science* **401**, 132–143.
- Yang, Q., Deng, Y. & Hu, W. 2009 Synthesis of alumina nanofibers by a mercury-mediated method. *Ceramics International* **35** (1), 531–535.

First received 11 May 2019; accepted in revised form 1 December 2019. Available online 5 February 2020